Compact Passive Components With Wide Stopband Using SIDGS Resonators

Deshan Tang, *Graduate Student Member, IEEE,* and Xun Luo, *Senior Member, IEEE*

***Abstract*—In this report, a series of substrate-integrated defected ground structure (SIDGS) resonators with wide stopband are proposed for the design of passive components. A tunable bandpass filter (BPF), a filtering balun, and an on-chip third-order filter are designed and fabricated based on the resonators. The center frequency of the tunable filter can be tuned from 1.75 to 2.7 GHz. The stopband can extend up to 9.5 GHz with a rejection level of 20 dB for all tuning cases. The filtering balun operates at 3.08 GHz with 3-dB FBW of 45%, which exhibits the in-band amplitude- and phase-imbalances of ±0.5 dB and ±0.4°, respectively. Meanwhile, the stopband extends to 18 GHz with the rejection level of 20 dB. The third-order filter operates at 28 GHz with the insertion loss of 2.9 dB and 3-dB FBW of 47%. The stopband extends to 170 GHz with the rejection level of 27 dB.**

***Index Terms*—Balun, substrate-integrated defected ground structure (SIDGS), tunable bandpass filter (BPF), wide stopband.**

I. Introduction

With the rapid development of modern wireless systems, the requirement of reconfigurability for a multi-mode operation becomes a major challenge for the circuit design. As crucial components in transceiver front ends, tunable bandpass filters (BPFs) and balun have aroused increasing interests [1]. However, relatively narrow stopband caused by the intrinsic harmonics of most reported structures limits the application. In this report, a series of passive components are proposed using substrate-integrated defected ground structure (SIDGS) resonators [2]–[5]. These passive components exhibit good in-band performance, wide stopband, wideband low radiation loss, and compact size.

II. Tunable BPF Using SIDGS

Fig. 1 shows the configuration of the proposed tunable filter, which is composed of two tunable SIDGS resonators, two feed-line with an interdigital capacitor, and four varactors [3]. Fig. 2 depicts the measured results of the fabricated BPF. The passband frequency can be tuned from 1.75 to 2.7 GHz with 3-dB FBW of 27.8% to 29.6% (Bias voltage variation: V_1 = 0 $\sim$ 15 V and V_2 = 2.3 $\sim$ 8 V). The return loss is better than 20 dB for the entire tuning range of the passband. The insertion loss varies from 1.1 to 1.9 dB. The stopband is better than 20 dB up to 9.5 GHz (i.e., $5.4f_{0L}$, where f_{0L} is the lower center frequency of the passband) in all tuning cases. The deviation between simulation and measurement is mainly due to the deviation from the model of varactors and capacitors in simulation and influence of welding. The TZ near 6.1 GHz may be generated by the bypass coupling of unexpected spurious resonant mode at 6.1 GHz. The core circuit size of the BPF is 7.8 mm × 8.7 mm (i.e., 0.07 λ_g × 0.08 λ_g, where λ_g is the microstrip guided wavelength at the lower center frequency of 1.75 GHz). The proposed tunable BPF exhibits enhanced performances on the low insertion loss, low return loss, wide stopband, and compact size.

The authors are with the Center for Advanced Semiconductor and Integrated Micro-System, University of Electronic Science and Technology of China, Chengdu 611731, China.

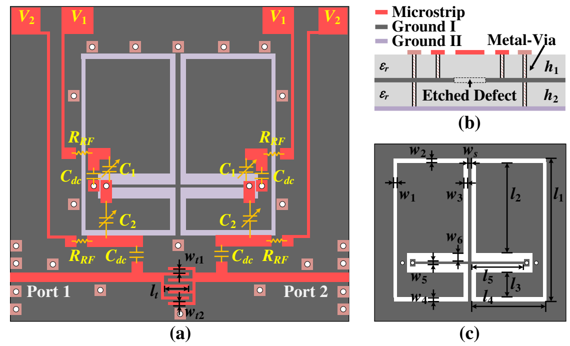

Fig. 1. (a) Configuration of the proposed tunable filter. (b) Layer diagram. (c) Details of the middle layer.

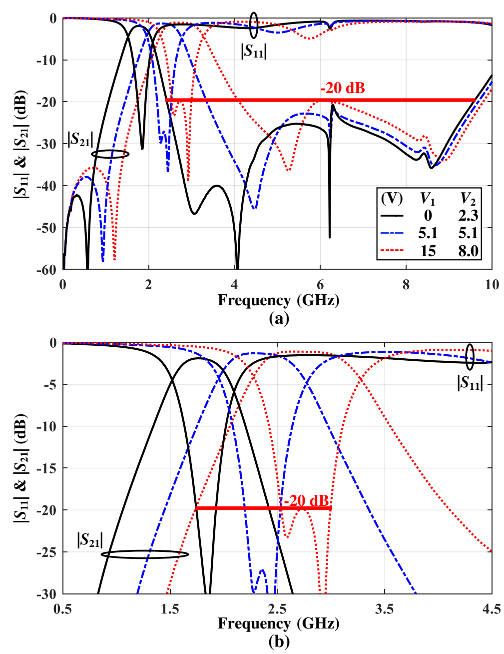

Fig. 2. Measured results of the developed tunable filter prototype. Bias voltage variation: V_1 = 0 $\sim$ 15 V and V_2 = 2.3 $\sim$ 8 V.

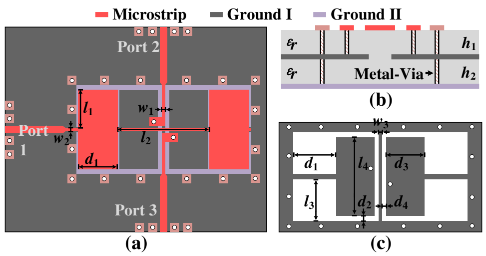

Fig. 3. Configuration of the proposed hybrid microstrip and SIDGS balun. (a) Top view. (b) Layer diagram. (c) Details of ground I.

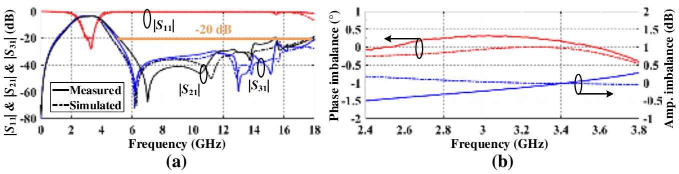

Fig. 4. Measured and simulated results of the proposed balun. (a) S-parameters. (b) In-band amplitude- and phase-imbalances.

III. Filtering Balun Using SIDGS

Fig. 3 depicts the configuration of the hybrid microstrip and SIDGS balun [4]. The balun is composed of two SIDGS resonators and a microstrip resonator, which are integrated at different layers with the surrounding ground and metal-vias. The simulated and measured results of S-parameters are depicted in Fig. 4. The center frequency of the balun is 3.08 GHz with the 3-dB FBW of 45%. The minimum in-band insertion loss is 0.6 dB excluding the theoretical 3-dB loss. The in-band amplitude- and phase-imbalances are $\pm$0.5 dB and $\pm0.4^\circ$, respectively. Meanwhile, the stopband is up to 18 GHz with a rejection level higher than 20 dB. The core size is about 0.12 $\lambda_g \times$ 0.2 λ_g, where λ_g is the microstrip guided wavelength at the center frequency.

IV. On-Chip Third-Order Filter Using SIDGS

To design a on-chip wideband third-order BPF, three stacked-coupled SIDGS resonators are used [5]. Such stacked-coupled scheme can reduce the size of the filter. The feed-lines are tapped to two resonators. Meanwhile, the cross coupling of two resonators are introduced by the parallel-plate capacitor. The configuration of the third-order BPF are shown in Fig. 5. The third-order BPF is fabricated in a standard 40-nm CMOS technology. The simulated and measured results of S-parameters are shown in Fig. 6. The center frequency of the BPF is 28 GHz with the 3-dB FBW of 47%. The minimum in-band insertion loss is 2.9 dB. The return loss is better than 15 dB in the simulated result. However, due to the deviation of the dielectric parameters between simulation and practical fabrication and the parasitic parameters of GSG pad, the measured return loss is worse than 10 dB. Meanwhile, the stopband is up to 170 GHz with a rejection level higher than 27 dB. The stopband $|S_{11}|$ is higher than -4 dB up to 155 GHz. In addition, the core circuit size of the BPF is 258 μm $\times$ 283 μm.

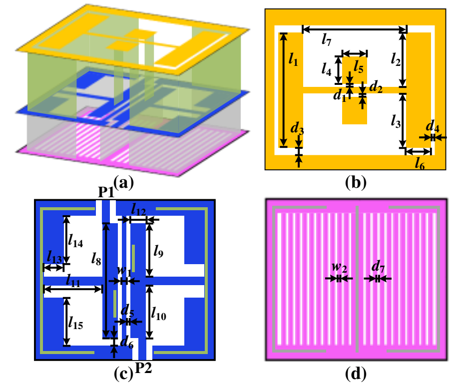

Fig. 5. (a) 3-D view of the third-order BPF. (b) Configuration of M8. (c) Configuration of V7 and M7. (d) Configuration of V6 and M6.

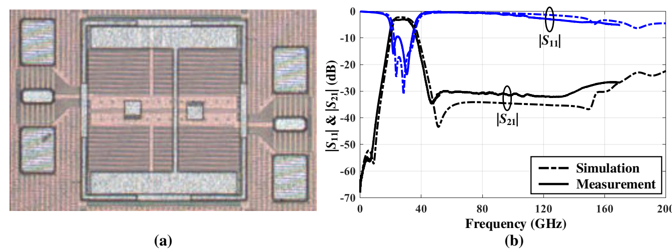

Fig. 6. (a) Photograph of the proposed third-order BPF. (b) Measured and simulated results of the proposed third-order BPF.

V. Conclusion

In this report, a series of SIDGS resonators are proposed. Based on the resonators, various passive components are designed, fabricated, and measured. The design prototypes show the merits of wide stopband, low insertion loss, and compact size.

VI. Acknowledgment and Next Plan

The IEEE MTT-S Undergraduate/Pregraduate Scholarship motivates and supports me to pursue research in the microwave, which is a great honor to me. In addition, I would like to thank my advisor Prof. dr. Xun Luo for the invaluable guidance. I will continue to study in this field and make further progress in providing efficient communication for humanity.

References

[1] R. Garg, I. Bahl, and M. Bozzi, *Microstrip lines and slotlines*, 3rd ed. Boston, MA, USA: Artech House, 2013.

[2] D. Tang, C. Han, Z. Deng, H. J. Qian, and X. Luo, "Substrate-integrated defected ground structure for single- and dual-band bandpass filters with wide stopband and low radiation loss," *IEEE Trans. Microw. Theory Techn.*, vol. 69, no. 1, pp. 659–670, Jan. 2021.

[3] D. Tang, H. J. Qian, Y. Dong, and X. Luo, "Compact 1.75–2.7 GHz tunable BPF with wide stopband up to 9.5 GHz using harmonic-controlled SIDGS resonators," *IEEE Trans. Circuits Syst. II, Exp. Briefs*, vol. 69, no. 11, pp. 4228–4232, Nov. 2022.

[4] D. Tang and X. Luo, "Compact filtering balun with wide stopband and low radiation loss using hybrid microstrip and substrate-integrated defected ground structure," *IEEE Microw. Wireless Compon. Lett.*, vol. 31, no. 6, pp. 549–552, Jun. 2021.

[5] D. Tang and X. Luo, "On-chip mm-wave second-/third-order BPF and balun with wide stopband and low radiation loss using SIDGS resonators in 40-nm CMOS," *IEEE Trans. Microw. Theory Techn.*, Early Access.